Physics Letters B 711 (2012) 301–306

Contents lists available at SciVerse ScienceDirect

Physics Letters B

www.elsevier.com/locate/physletb

Elliptic and triangular flow and their correlation in ultrarelativistic high multiplicity proton–proton collisions at 14 TeV

Wei-Tian Deng [a], Zhe Xu [a,b,c,*], Carsten Greiner [b]

[a] Frankfurt Institute for Advanced Studies (FIAS), Ruth-Moufang-Strasse 1, 60438 Frankfurt am Main, Germany
[b] Institut für Theoretische Physik, Johann Wolfgang Goethe-Universität Frankfurt, Max-von-Laue-Strasse 1, 60438 Frankfurt am Main, Germany
[c] Department of Physics, Tsinghua University, Beijing 100084, China

ARTICLE INFO

Article history:
Received 21 December 2011
Received in revised form 17 February 2012
Accepted 6 April 2012
Available online 10 April 2012
Editor: J.-P. Blaizot

ABSTRACT

The spatial configuration of initial partons in high multiplicity proton–proton scatterings at 14 TeV is assumed as three randomly positioned "hot spots". The parton momentum distribution in the hot spots is calculated by HIJING2.0 with some modifications. This initial condition causes not only large eccentricity ϵ_2 but also triangularity ϵ_3 and the correlation of $\epsilon_2 - \epsilon_3$ event-plane angles. The final elliptic flow v_2, triangular flow v_3, and the correlation of $v_2 - v_3$ event-plane angles are calculated by using the parton cascade model BAMPS to simulate the space–time parton evolution. Our results show that the $v_2 - v_3$ correlation is different from that of $\epsilon_2 - \epsilon_3$. This finding indicates that translations of different Fourier components of the initial spatial asymmetry to the final flow components are not independent. A dynamical correlation between the elliptic and triangular flow appears during the collective expansion.

1. Introduction

A strong interest in high multiplicity events in ultrarelativistic proton–proton collisions has arisen recently, since a near side "ridge" has been found in such events by the CMS Collaboration at the Large Hadron Collider (LHC) at $\sqrt{s} = 7$ TeV [1]. This phenomenon is very similar to that observed in Au–Au collisions at the Relativistic Heavy Ion Collider (RHIC) at $\sqrt{s_{NN}} = 0.2$ TeV [2–4]. Because the Quark–Gluon Plasma (QGP) created at RHIC behaves like a nearly perfect fluid [5], one may suppose that a similar hydrodynamic behaviour has appeared in high multiplicity p–p collisions at LHC [6]. Methods developed to investigate QGP at RHIC can be used to predict new phenomena in p–p collisions at LHC. In this work we are concentrating on the elliptic and triangular flow induced by the initial eccentricity and triangularity in ultrarelativistic high multiplicity p–p collisions at the highest LHC energy.

The elliptic flow parameter v_2 is the best experimental observable determining the strength of the hydrodynamic collectivity [7–10]. In the presence of strong interactions of system constituents, v_2 is obtained by the translation of the spatial asymmetry of initially produced matter into the final particle angular distribution [11,12]. There are two ways to make a spatial asymmetry in nucleus–nucleus collisions. One is the geometric overlap in non-central collisions. This has been adopted to p–p collisions at LHC, because a proton also has its extension though small. However, the predictions following the geometric overlap-eccentricity ϵ_2 showed small values of the elliptic flow parameter $v_2 \approx 3\%$ in minimum bias, either in hydrodynamic calculations [13–15] or in the $\epsilon_2 - v_2$ scaling [16,17]. The latter is assumed to be the same as that proposed for nucleus–nucleus collisions at RHIC [18,19]. In the geometric picture non-central collisions provide large initial eccentricity, which is the necessary condition for large elliptic flow. However, the particle multiplicity in such collisions in the case of p–p scatterings is rather low. Non-flow effects can be hardly eliminated.

The second source of a spatial asymmetry comes from statistical density fluctuations of the initially produced matter on the event-by-event basis [20]. This is the reason for the nonvanishing v_2 (and also higher harmonics) in central nucleus–nucleus collisions at LHC [21]. Due to the much smaller volume of a proton compared with an Au nucleus, it is natural to consider fluctuations in central p–p collisions at the LHC energy, which can provide both initial eccentricity and high multiplicity. A few hot spots or flux tubes may be excited in a p–p collision and lead to measurable elliptic flow at LHC [22–25]. Moreover, parton evolutions and multiple scatterings [26,27] can also generate large event-by-event fluctuations.

Unlike the smooth initial distribution that generates only even-order Fourier components in the momentum angular distribution, initial fluctuations lead to nonvanishing odd-order components, which are shown to contribute the azimuthal correlations observed

* Corresponding author at: Department of Physics, Tsinghua University, Beijing 100084, China.
E-mail address: xuzhe@mail.tsinghua.edu.cn (Z. Xu).

0370-2693/$ – see front matter
http://dx.doi.org/10.1016/j.physletb.2012.04.010

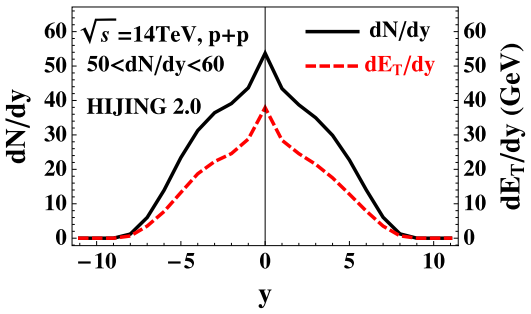

Fig. 1. (Color online.) The rapidity distribution of multiplicity and transverse energy of hadrons produced in high multiplicity p + p collisions at 14 TeV, calculated by HIJING2.0 [40].

at RHIC [28–31]. In particular, the triangular flow v_3 from the initial triangularity ϵ_3 is intensively studied in the recent works [32–38]. In central Au + Au collisions v_3 is as large as v_2 [37].

For p–p collisions at LHC we suggest that v_3 is as important as v_2 in high multiplicity events. Different from Au + Au collisions at RHIC, where calculations [33,20] indicate no correlations between the initial event-plane angles of ϵ_2 and ϵ_3 and between the final event-plane angles of v_2 and v_3, such correlations could exist in the p–p collisions at LHC due to the smaller number of hot spots. Measurements on the flow correlations will shed light on details in the context of collective flow phenomena. In this work we calculate ϵ_2, ϵ_3, v_2, v_3, and their correlations. The event-by-event generation of the parton initial conditions is an implementation of the hot spots scenario [23] by using the recent version of HIJING2.0 [39–41]. The dynamical space–time evolution is calculated by using the parton cascade BAMPS [42].

2. Initial conditions

HIJING [39–41] is a Monte Carlo event generator for hadron productions in high energy nucleon–nucleon, nucleon–nucleus, and nucleus–nucleus collisions. It is essentially a two-component model, which describes the production of hard parton jets and the soft interaction between nucleon remnants. While the hard jets production can be calculated by perturbative QCD (pQCD), nucleon remnants interact via soft gluon exchanges described by the string model [43]. The produced hard jet pairs and the two excited remnants are treated as independent strings, which fragment to resonances that decay to final hadrons. The predictions using the updated HIJING2.0 [40] are in good agreements with the recently measured hadron spectra at LHC in p + p collisions at $\sqrt{s} = 0.9$, 2.36 and 7 TeV [44–48], and central Pb + Pb collisions at $\sqrt{s_{NN}} = 2.76$ TeV [49].

Using HIJING2.0 we calculate the hadron multiplicity for p + p collisions at 14 TeV and find that the total hadron multiplicity dN/dy at $y = 0$ has a mean value of 10.4 and possesses a high multiplicity tail reaching the abundance of semi-peripheral Cu + Cu collisions at $\sqrt{s_{NN}} = 62.4$ GeV at RHIC [50]. In this work we are interested in the events in the window of $50 < dN/dy(y = 0) < 60$. In these events the probability to produce three strings (one is formed by the hard jet pairs and other two from the excited remnants) is more than 80%. We thus neglect, for simplicity, events without hard jets (17%) and events containing more than one jet string (3%). The rapidity distributions of the hadron multiplicity and transverse energy in these selected events are shown in Fig. 1. The peak at midrapidity is due to the fact that in the selected events, the hard jets production and the multiple gluons exchange in the soft interaction mostly occur at midrapidity.

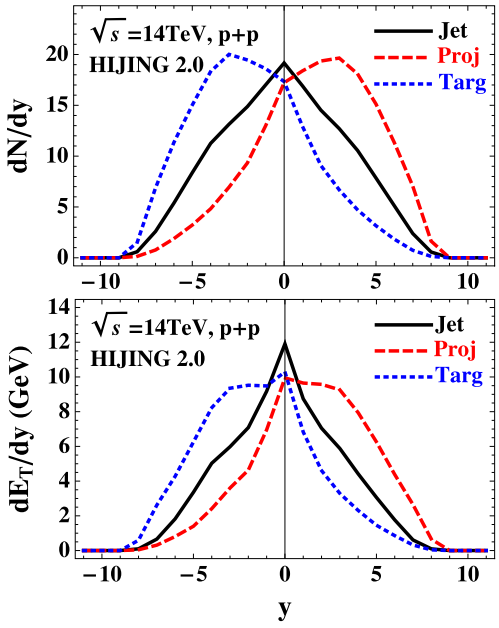

Fig. 2. (Color online.) The same as Fig. 1, but on the parton level from three strings. See details in text.

To generate the initial condition on the parton level, we turn off the resonance decays in HIJING and return to the representation of resonances by quark–antiquark pairs or quark–diquark pairs according to the LUND string breaking [51,43]. This approach is similar to the string melting implemented in AMPT [52], where final hadrons are converted into partons. Fig. 2 shows the rapidity distribution of parton number and transverse energy from jet, projectile, and target string, respectively.

Because the three strings break independently, we assume that partons from each string build a hot spot. Due to the high collider energy all partons are produced at $z = 0$. The spatial distribution of the three hot spots in the transverse plane follows the scenario proposed in Ref. [23]. The center of the hot spots is determined according to the proton spatial density [53]

$$n_p(r) = \frac{n_0}{1 + e^{(r-R_0)/d}}, \tag{1}$$

where $n_0 = 0.17/\text{fm}^3$, $R_0 = 0.56$ fm and $d = 0.112$ fm. The spatial parton distribution in each hot spot is assumed to have a Gaussian profile e^{-r^2/r_0^2}, where r_0 gives the size of the hot spots.

Because the partons from the two remnant strings are soft, the size r_0 of the two hot spots for the remnants could be larger than that for the jet string. However, we assume that r_0 is equal for all hot spots, which gives the largest effect on the initial asymmetry. r_0 is set to be 0.2 fm. The smaller the r_0, the larger the ϵ_2 and ϵ_3 [23].

Translating particles into the frame where the average position is equal zero, i.e., $\langle x \rangle = \langle y \rangle = 0$, the harmonic components ϵ_n of the spatial azimuthal distribution are defined as [33]

$$\epsilon_n = \frac{\sqrt{\langle r^n \cos(n\phi)\rangle^2 + \langle r^n \sin(n\phi)\rangle^2}}{\langle r^n \rangle}, \tag{2}$$

where r, ϕ are parton polar coordinates. The corresponding initial event-plane angles are given by

$$\Phi_n = \frac{1}{n} \arctan \frac{\langle r^n \sin(n\phi)\rangle}{\langle r^n \cos(n\phi)\rangle}. \tag{3}$$

These are the angles $\Phi = \Phi_n$ where $\langle -r^n \cos n(\phi - \Phi)\rangle / \langle r^n \rangle$ has the maximum, which is ϵ_n [see Eq. (2)]. For instance, for an

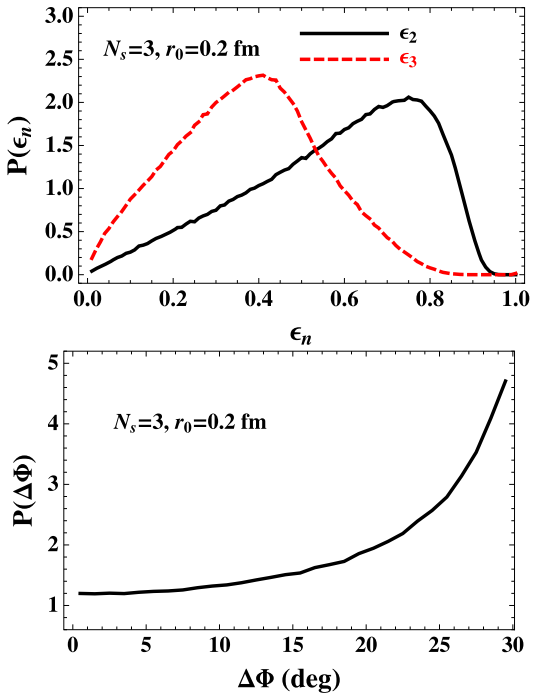

Fig. 3. (Color online.) Upper: the probability distribution of spatial eccentricity and triangularity. Lower: correlation (arbitrary unit) of the $\epsilon_2 - \epsilon_3$ event-plane angles. N_s denotes the number of the hot spots.

ellipse shape with the short axis in the x direction $\Phi_2 = 0$ and $\epsilon_2 = \langle y^2 - x^2\rangle/\langle y^2 + x^2\rangle$. Our definition of Φ_n differs from that from Ref. [33] by $\pm\pi/n$.

The upper panel of Fig. 3 shows the probabilities of the eccentricity ϵ_2 and the triangularity ϵ_3 in the high multiplicity p + p collisions at 14 TeV on the event-by-event basis. The parton number in each hot spot is set to be 100. Using exact numbers from HIJING (about 160 in each hot spot taken over all rapidities, see Fig. 2) has tiny changes on the results. 100 partons per hot spot are roughly the numbers within the rapidity range $|y| < 2.5$, which is a similar region covered in CMS [1]. Our results show that the most ϵ_3 are not much smaller than the most ϵ_2, which indicates the possibility to measure both v_2 and v_3 experimentally, if the assumptions of the initial condition and the hydrodynamic transport are justified.

Due to the random nature of the initial condition, the distribution of Φ_2 and Φ_3 are uniform within the interval of $[-\pi/2, \pi/2]$ and $[-\pi/3, \pi/3]$, respectively. The lower panel of Fig. 3 shows the probability distribution of the angle difference, $\Delta\Phi = |\Phi_2 - \Phi_3|$, which indicates the correlation of the two initial event-planes. Events with $\Delta\Phi = 30$ degree are more probable.

For initial conditions with two hot spots instead of three, we expect vanishing ϵ_3. With four or more hot spots both ϵ_3 and ϵ_2 become smaller and their event-plane angles will be less correlated. Therefore, the largest correlation comes from events with three hot spots.

When hot spots expand and overlap, collective flow components in higher order will be built up. By analogy with ϵ_n flow coefficients v_n are defined as the harmonic components of the particle azimuthal distribution in momentum space

$$\frac{dN}{d^2p_T\,dy} = \frac{1}{2\pi}\frac{dN}{p_T\,dp_T\,dy}\left[1 + 2\sum_n v_n \cos n(\psi - \Psi_n)\right] \tag{4}$$

where

$$v_n(p_T) = \langle \cos n(\psi - \Psi_n)\rangle, \tag{5}$$

$$\Psi_n = \frac{1}{n}\arctan\frac{\langle \sin(n\psi)\rangle}{\langle \cos(n\psi)\rangle}. \tag{6}$$

Ψ_n is the event-plane angle [54], i.e., $\langle \cos n(\psi - \Psi)\rangle$ at $\Psi = \Psi_n$ has the maximum, which is v_n.

If the translations from ϵ_n to v_n for all components are completely independent, we will obtain $\Psi_n = \Phi_n$. The strong correlation of $\Delta\Phi$ seen in Fig. 3 will be observed in $\Delta\Psi = |\Psi_2 - \Psi_3|$ too. If such correlation can be measured experimentally at LHC, this will be the evidence for the hot spot scenario of the initial condition and the hydrodynamic behaviour of the parton matter in high multiplicity p + p collisions. In this work we discuss this issue by simulating the parton collectivity within a microscopic manner.

3. Elliptic, triangular flow and their correlation

The space–time evolution of the partons is simulated by the parton cascade model BAMPS (Boltzmann Approach of MultiParton Scatterings) [42], which solves the Boltzmann equation for on-shell partons. For simplicity we regard partons, which stem from the string breaking (see Section 2), as identical massless Boltzmann particles. The particle degeneracy factor is assumed to be the same as that of gluons together with quarks with two flavours. This leads to the particle number density $n_{eq} = (40/\pi^2)T^3$, where T is the temperature, if the system is in local thermal and chemical equilibrium. Furthermore, we consider only elastic binary scatterings and assume the isotropic distribution of the collision angle.

The Boltzmann equation applies for systems when the particle mean free path $\lambda_{mfp} = 1/(n\sigma)$ is larger than the mean particle distance $d = n^{-1/3}$, where n is the local particle number density. For chosen constant λ_{mfp}/d ratio as a global parameter we determine the total cross sections σ in local cells, which are used to simulate scatterings [42].

To assess hydrodynamic behaviour of the partons considered in this work we calculate the shear viscosity to the entropy density ratio η/s for given λ_{mfp}/d ratio. The shear viscosity is proportional to the energy density and the mean free path [55], $\eta = (2/5)e\lambda_{mfp}$. Assuming local thermal equilibrium, the entropy density is $s = (4 - \ln\lambda_p)n$, where $\lambda_p = n/n_{eq}$ denotes the particle fugacity. We have then $\eta/s = 0.752\lambda_{mfp}/d/(4 - \ln\lambda_p)/\lambda_p^{1/3}$. The relation $e = 3nT$ is used in the last equation. The ratio η/s has a weak dependence on the fugacity. Therefore, we take $\eta/s = 0.188\lambda_{mfp}/d$, which is exact for $\lambda_p = 1$, as an estimate of the η/s value for systems out of equilibrium, such as the present case. For choosing $\lambda_{mfp}/d = 2$ for instance we obtain $\eta/s \approx 0.376$.

Further model parameters are set as follows: The initial time for starting BAMPS is 0.1 fm/c. Before that time partons propagate freely. The cell length in the transverse plane is $\Delta x = \Delta y = 0.02$ fm, while the longitudinal cell size is $\Delta\eta \approx 0.1$, expressed in the space–time rapidity $\eta = 0.5\ln[(t + z)/(t - z)]$. The test particle method [42] is used to enhance the numerical accuracy. For that the parton density is amplified by a factor of 3000. Cross sections are reduced by the same factor to keep the mean free path unchanged. This means that in one BAMPS run there are 3000 back-to-back jet pairs located in one hot spot. Their spatial orientations are randomly sampled, which minimizes the non-flow effects. Parton scatterings stop when the local energy density is lower than 1 GeV/fm^3. This mimics the phase transition, which has to be implemented in BAMPS in the future. For the event-by-event analysis we compute ten thousands runs. The elliptic and triangular flow, and the corresponding event-plane angles in each run are calculated by collecting partons at midrapidity $y \in [-0.5 : 0.5]$ with $y = 0.5\ln[(E + p_z)/(E - p_z)]$.

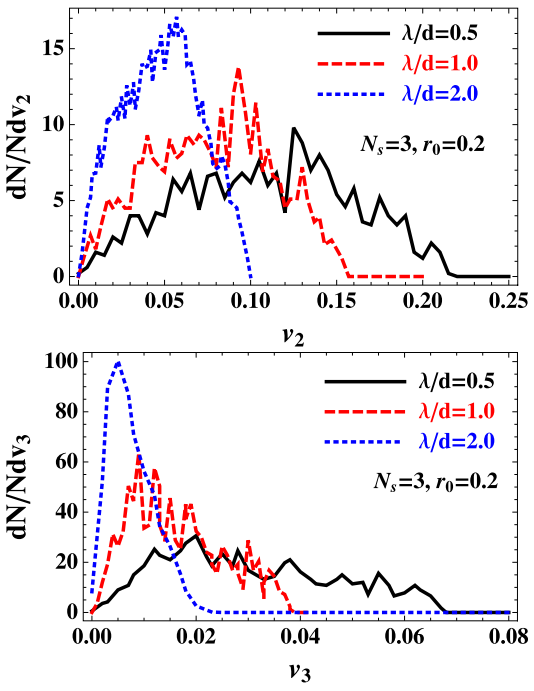

Fig. 4. (Color online.) Event-by-event distribution of v_2 and v_3.

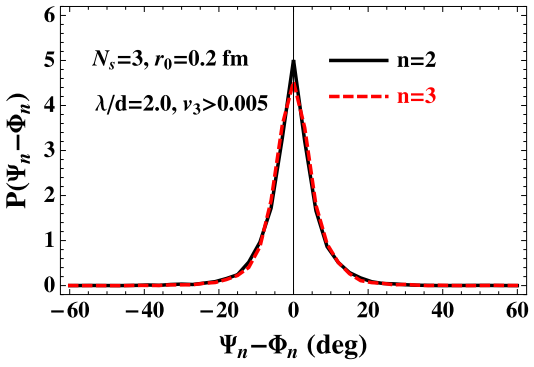

Fig. 5. (Color online.) Distributions (arbitrary unit) of the difference between the initial event-plane angle Φ_n and corresponding final one Ψ_n.

Fig. 4 shows the event-by-event distribution of the p_T-averaged v_2 and v_3. For $\lambda_{mfp}/d = 2$, v_2 has a broad distribution between 0 and 0.1 with the maximum at 0.06, which is comparable with the values at RHIC. v_3's distribution is narrow and centered at 0.01. For smaller λ_{mfp}/d ratios the viscous effect becomes smaller and the collective flow becomes stronger. The value of v_2 and v_3 can reach 0.2 and 0.07, respectively, for $\lambda_{mfp}/d = 0.5$, which corresponds to $\eta/s \approx 0.094$. Therefore, if the parton matter in high multiplicity p + p events at LHC has a small η/s ratio, both v_2 and v_3 are measurable quantities. Although the Boltzmann equation is not strictly valid for systems with $\lambda_{mfp}/d < 1$, its solution agrees well with results from hydrodynamic calculations with corresponding η/s ratio [56].

We are more interested in the translation from the initial spatial asymmetry to the final collective flow. In Fig. 5 we show the distributions of the difference between Ψ_n and Φ_n for $n = 2, 3$ [see the definitions in Eqs. (3) and (6)]. The distributions of $n = 2, 3$ are almost the same. They peak at zero and have a form looking like the Dirac delta function. It seems that translations from ϵ_2 to v_2 and from ϵ_3 to v_3 take place independently.

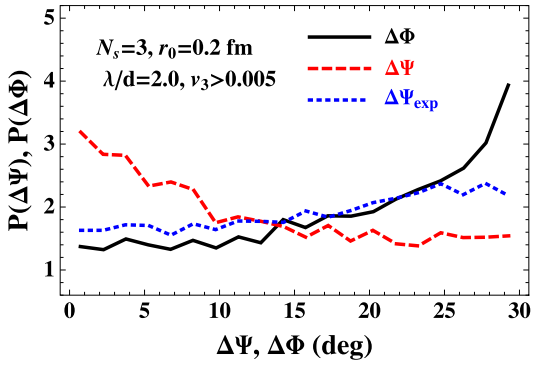

Fig. 6. (Color online.) Correlations (arbitrary unit) of initial $\epsilon_2 - \epsilon_3$ and final $v_2 - v_3$ event-plane angles. The dotted curve is obtained by independent samplings of Ψ_2 and Ψ_3 according to Fig. 5. Events with $v_3 > 0.005$ are selected.

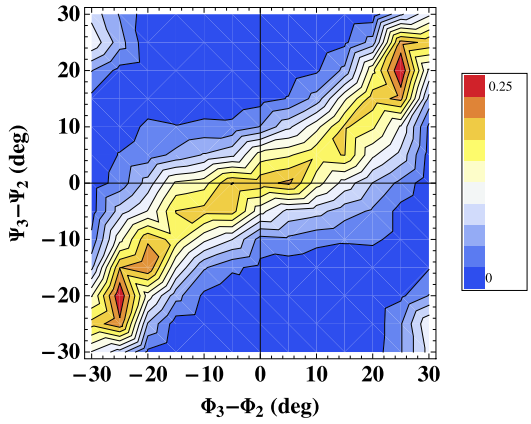

Fig. 7. (Color online.) Contour plot $d^2N/d(\Phi_3 - \Phi_2)/d(\Psi_3 - \Psi_2)$ (arbitrary unit).

However, the event-plane correlations present a different picture, which is given in Fig. 6. We have selected events with $v_3 > 0.005$, because in events with $v_3 < 0.005$, Ψ_3 (possibly also Φ_3 due to tiny ϵ_3) is a random number within $[-\pi/3, \pi/3]$ and has no correlation with the initial Φ_3. The solid curve shows the angular correlations of the initial $\epsilon_2 - \epsilon_3$ event-planes, which is almost the same as the one demonstrated with a simpler initial condition, seen in Fig. 3. The dashed curve shows the corresponding correlation of the $v_2 - v_3$ event-planes after parton cascade simulations. Surprisingly, the $v_2 - v_3$ event-plane correlation function has a maximum at zero degree and, thus, is totally different from the $\epsilon_2 - \epsilon_3$ one. With the same event-by-event initial conditions but without parton cascade simulations we sample Ψ_2 and Ψ_3 independently according to Fig. 5. The result is plotted by the dotted curve in Fig. 6, which shows, as expected, the same trend as the initial angular correlation, although the correlation is weaker due to the width in the distributions seen in Fig. 5. Because the independent samplings of Ψ_2 and Ψ_3 does not reproduce the $\Psi_2 - \Psi_3$ correlation (dashed curve) in the parton cascade calculations, we conclude that elliptic and triangular flow are correlated during the dynamical expansion. This dynamical correlation seems to rotate different event-planes (30 degree in $\Delta\Phi$) to a unified event-plane (0 degree in $\Delta\Psi$).

To convince ourselves of the finding, we show the contour plot $d^2N/d(\Phi_3 - \Phi_2)/d(\Psi_3 - \Psi_2)$ in Fig. 7. Integral over $\Psi_3 - \Psi_2$ gives the solid curve in Fig. 6, while integral over $\Phi_3 - \Phi_2$ gives the dashed curve in Fig. 6. The difference between the solid and the dashed curve in Fig. 6 is reflected in the asymmetry in Fig. 7 along the plane $\Psi_3 - \Psi_2 = \Phi_3 - \Phi_2$. At a fixed $\Phi_3 - \Phi_2$, $\Psi_3 - \Psi_2$ has a broad distribution with a center moving toward $\Psi_3 - \Psi_2 = 0$.

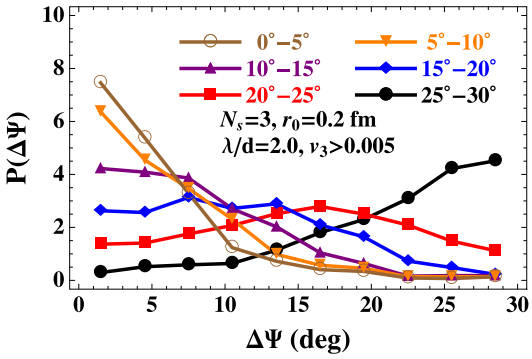

Fig. 8. (Color online.) Correlations (arbitrary unit) of final $v_2 - v_3$ event-plane angles within the separate bins of the initial correlation angles, $|\Phi_2 - \Phi_3| = 0$–5, 5–10, 10–15, 15–20, 20–25, and 25–30 degree.

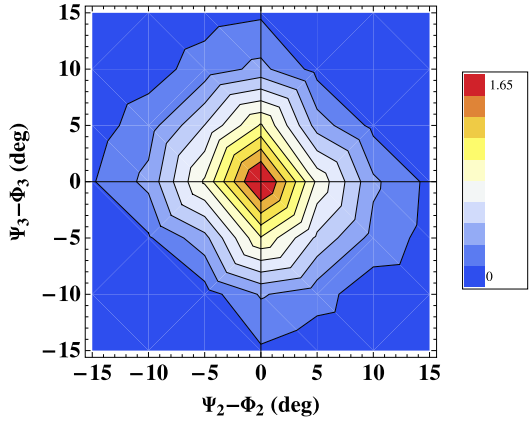

Fig. 9. (Color online.) Contour plot $d^2N/d(\Psi_2 - \Phi_2)/d(\Psi_3 - \Phi_3)$ (arbitrary unit).

This is better observed in Fig. 8, where the final $|\Psi_2 - \Psi_3|$ correlations from events within separate bins of the initial correlation angles, $|\Phi_2 - \Phi_3| = 0$–5, 5–10, 10–15, 15–20, 20–25, and 25–30 degree, are shown. We clearly see strong broadening of all the distributions toward zero degree. For instance, we choose the curve denoted by 10–15 degree. When assuming independent translations from ϵ_n to v_n, this curve is expected to peak at 10–15 degree. However, we realize its maximum at zero degree.

Fig. 9 shows another contour plot $d^2N/d(\Psi_2 - \Phi_2)/d(\Psi_3 - \Phi_3)$. Integral over $\Psi_3 - \Phi_3$ (or $\Psi_2 - \Phi_2$) gives the solid (or dashed) curve in Fig. 5. If $\Psi_2 - \Phi_2$ and $\Psi_3 - \Phi_3$ are independent, the contour structure should be symmetric along the planes $\Psi_2 - \Phi_2 = 0$ and $\Psi_3 - \Phi_3 = 0$. It is not the case. Assuming $\Phi_2 = 0$ and $\Phi_3 = 30$ degree (which are more favored), and choosing a Ψ_2 with $\Psi_2 - \Phi_2 > 0$, we see from the contour plot that events with $\Psi_3 - \Phi_3 < 0$ are more favored. This indicates that the angle between Ψ_2 and Ψ_3 is smaller than 30 degree and the two event-planes rotate toward each other during the dynamical expansion.

We have to note that our conclusion on the dynamical correlation between v_2 and v_3 needs further verifications, because the fluctuating initial configuration of hot spots may affect the final event-plane angular correlation. It is worthwhile to study this issue for a smooth initial condition with few components ϵ_n and given initial event-plane angular correlation. We leave this as a task for a future investigation.

4. Conclusions

In this work we have calculated the elliptic and triangular flow in high multiplicity proton–proton collisions at the LHC energy 14 TeV. The reason for the measurable flows is the assumed initial fluctuation in the hot spot scenario. The motivation of this work was to find final $v_2 - v_3$ event-plane correlation expected by the initial $\epsilon_2 - \epsilon_3$ event-plane correlation. The latter exists for the assumed initial condition with three statistically distributed hot spots originating from three independent fragmenting strings in p + p collisions modelled by HIJING. The results obtained by using parton transport model BAMPS showed the largest $v_2 - v_3$ event-plane angular correlation at zero degree, which is the opposite to the expectation at 30 degree. This observation indicates a dynamical correlation between elliptic and triangular flow during the expansion. Their event-planes rotate toward each other. If so, any initial correlations will be washed out and it is more difficult to extract initial conditions from the flow observations. On the other hand, because we do not expect initial event-plane angular correlations in nucleus–nucleus collisions at RHIC and LHC, measurements on the final harmonic flow event-plane angular correlations in these experiments would confirm our conclusion, if data favor zero degree correlation of v_2, v_3 event-plane angles. The correlation of different flow components is a new finding and needs further verifications in the future.

Acknowledgements

W.-T.D. would like to acknowledge J. Casalderrey-Solana, Y.-K. Song and X.-N. Wang for useful discussions. Z.X. thanks S. Esumi for his fruitful suggestions. The BAMPS simulations were performed at the Center for Scientific Computing of Goethe University. This work was financially supported by the Helmholtz International Center for FAIR within the framework of the LOEWE program launched by the State of Hesse.

References

[1] V. Khachatryan, et al., CMS Collaboration, JHEP 1009 (2010) 091, arXiv:1009.4122 [hep-ex].
[2] J. Adams, et al., STAR Collaboration, Phys. Rev. Lett. 95 (2005) 152301, arXiv:nucl-ex/0501016.
[3] A. Adare, et al., PHENIX Collaboration, Phys. Rev. C 78 (2008) 014901, arXiv:0801.4545 [nucl-ex].
[4] B. Alver, et al., PHOBOS Collaboration, J. Phys. G 35 (2008) 104080, arXiv:0804.3038 [nucl-ex].
[5] P. Huovinen, P.F. Kolb, U.W. Heinz, P.V. Ruuskanen, S.A. Voloshin, Phys. Lett. B 503 (2001) 58, arXiv:hep-ph/0101136.
[6] K. Werner, I. Karpenko, T. Pierog, Phys. Rev. Lett. 106 (2011) 122004, arXiv:1011.0375 [hep-ph].
[7] I. Arsene, et al., BRAHMS Collaboration, Nucl. Phys. A 757 (2005) 1, arXiv:nucl-ex/0410020.
[8] B.B. Back, et al., Nucl. Phys. A 757 (2005) 28, arXiv:nucl-ex/0410022.
[9] J. Adams, et al., STAR Collaboration, Nucl. Phys. A 757 (2005) 102, arXiv:nucl-ex/0501009.
[10] K. Adcox, et al., PHENIX Collaboration, Nucl. Phys. A 757 (2005) 184, arXiv:nucl-ex/0410003.
[11] J.Y. Ollitrault, Phys. Rev. D 46 (1992) 229.
[12] S. Voloshin, Y. Zhang, Z. Phys. C 70 (1996) 665, arXiv:hep-ph/9407282 [hep-ph].
[13] M. Luzum, P. Romatschke, Phys. Rev. Lett. 103 (2009) 262302, arXiv:0901.4588 [nucl-th].
[14] S.K. Prasad, V. Roy, S. Chattopadhyay, A.K. Chaudhuri, Phys. Rev. C 82 (2010) 024909, arXiv:0910.4844 [nucl-th].
[15] G. Ortona, G.S. Denicol, P. Mota, T. Kodama, arXiv:0911.5158 [hep-ph].
[16] L. Cunqueiro, J. Dias de Deus, C. Pajares, Eur. Phys. J. C 65 (2010) 423, arXiv:0806.0523 [hep-ph].
[17] D. d'Enterria, G.K. Eyyubova, V.L. Korotkikh, I.P. Lokhtin, S.V. Petrushanko, L.I. Sarycheva, A.M. Snigirev, Eur. Phys. J. C 66 (2010) 173, arXiv:0910.3029 [hep-ph].
[18] R.S. Bhalerao, J.P. Blaizot, N. Borghini, J.Y. Ollitrault, Phys. Lett. B 627 (2005) 49, arXiv:nucl-th/0508009.
[19] H.J. Drescher, A. Dumitru, C. Gombeaud, J.Y. Ollitrault, Phys. Rev. C 76 (2007) 024905, arXiv:0704.3553 [nucl-th].
[20] Z. Qiu, U.W. Heinz, Phys. Rev. C 84 (2011) 024911, arXiv:1104.0650 [nucl-th].
[21] K. Aamodt, et al., ALICE Collaboration, Phys. Rev. Lett. 107 (2011) 032301, arXiv:1105.3865 [nucl-ex].

[22] P. Bozek, Acta Phys. Polon. B 41 (2010) 837, arXiv:0911.2392 [nucl-th].
[23] J. Casalderrey-Solana, U.A. Wiedemann, Phys. Rev. Lett. 104 (2010) 102301, arXiv:0911.4400 [hep-ph].
[24] A.K. Chaudhuri, Phys. Lett. B 692 (2010) 15, arXiv:0912.2578 [nucl-th].
[25] D.-M. Zhou, Y.-L. Yan, B.-G. Dong, X.-M. Li, D.-J. Wang, X. Cai, B.-H. Sa, Nucl. Phys. A 860 (2011) 68, arXiv:1012.1931 [nucl-th].
[26] T. Pierog, S. Porteboeuf, I. Karpenko, K. Werner, arXiv:1005.4526 [hep-ph].
[27] E. Avsar, C. Flensburg, Y. Hatta, J.-Y. Ollitrault, T. Ueda, Phys. Lett. B 702 (2011) 394, arXiv:1009.5643 [hep-ph].
[28] J. Takahashi, B.M. Tavares, W.L. Qian, R. Andrade, F. Grassi, Y. Hama, T. Kodama, N. Xu, Phys. Rev. Lett. 103 (2009) 242301, arXiv:0902.4870 [nucl-th].
[29] P. Sorensen, J. Phys. G 37 (2010) 094011, arXiv:1002.4878 [nucl-ex].
[30] B. Alver, G. Roland, Phys. Rev. C 81 (2010) 054905;
B. Alver, G. Roland, Phys. Rev. C 82 (2010) 039903 (Erratum), arXiv:1003.0194 [nucl-th].
[31] J. Xu, C.M. Ko, Phys. Rev. C 83 (2011) 021903, arXiv:1011.3750 [nucl-th];
J. Xu, C.M. Ko, Phys. Rev. C 84 (2011) 014903, arXiv:1103.5187 [nucl-th].
[32] B.H. Alver, C. Gombeaud, M. Luzum, J.Y. Ollitrault, Phys. Rev. C 82 (2010) 034913, arXiv:1007.5469 [nucl-th].
[33] H. Petersen, G.-Y. Qin, S.A. Bass, B. Muller, Phys. Rev. C 82 (2010) 041901, arXiv:1008.0625 [nucl-th].
[34] G.-Y. Qin, H. Petersen, S.A. Bass, B. Muller, Phys. Rev. C 82 (2010) 064903, arXiv:1009.1847 [nucl-th].
[35] B. Schenke, S. Jeon, C. Gale, Phys. Rev. Lett. 106 (2011) 042301, arXiv:1009.3244 [hep-ph].
[36] D. Teaney, L. Yan, Phys. Rev. C 83 (2011) 064904, arXiv:1010.1876 [nucl-th].
[37] G.-L. Ma, X.-N. Wang, Phys. Rev. Lett. 106 (2011) 162301, arXiv:1011.5249 [nucl-th].
[38] H. Petersen, C. Greiner, V. Bhattacharya, S.A. Bass, arXiv:1105.0340 [nucl-th].
[39] X.N. Wang, M. Gyulassy, Phys. Rev. D 44 (1991) 3501.
[40] W.-T. Deng, X.-N. Wang, R. Xu, Phys. Rev. C 83 (2011) 014915, arXiv:1008.1841 [hep-ph].
[41] W.-T. Deng, X.-N. Wang, R. Xu, Phys. Lett. B 701 (2011) 133, arXiv:1011.5907 [nucl-th].
[42] Z. Xu, C. Greiner, Phys. Rev. C 71 (2005) 064901, arXiv:hep-ph/0406278;
Z. Xu, C. Greiner, Phys. Rev. C 76 (2007) 024911, arXiv:hep-ph/0703233;
Z. Xu, C. Greiner, H. Stocker, Phys. Rev. Lett. 101 (2008) 082302, arXiv:0711.0961 [nucl-th];
Z. Xu, C. Greiner, Phys. Rev. C 79 (2009) 014904, arXiv:0811.2940 [hep-ph].
[43] T. Sjostrand, M. van Zijl, Phys. Rev. D 36 (1987) 2019;
T. Sjostrand, Comput. Phys. Commun. 39 (1986) 347.
[44] K. Aamodt, et al., ALICE Collaboration, Eur. Phys. J. C 65 (2010) 111, arXiv:0911.5430 [hep-ex].
[45] K. Aamodt, et al., ALICE Collaboration, Eur. Phys. J. C 68 (2010) 345, arXiv:1004.3514 [hep-ex].
[46] K. Aamodt, et al., ALICE Collaboration, Phys. Lett. B 693 (2010) 53, arXiv:1007.0719 [hep-ex].
[47] V. Khachatryan, et al., CMS Collaboration, JHEP 1002 (2010) 041, arXiv:1002.0621 [hep-ex].
[48] V. Khachatryan, et al., CMS Collaboration, Phys. Rev. Lett. 105 (2010) 022002, arXiv:1005.3299 [hep-ex].
[49] B. Abelev, et al., ALICE Collaboration, Phys. Rev. Lett. 105 (2010) 252301, arXiv:1011.3916 [nucl-ex].
[50] B. Alver, et al., PHOBOS Collaboration, Phys. Rev. Lett. 98 (2007) 242302, arXiv:nucl-ex/0610037.
[51] B. Andersson, G. Gustafson, B. Nilsson-Almqvist, Nucl. Phys. B 281 (1987) 289;
B. Nilsson-Almqvist, E. Stenlund, Comput. Phys. Commun. 43 (1987) 387.
[52] Z.-w. Lin, C.M. Ko, Phys. Rev. C 65 (2002) 034904, arXiv:nucl-th/0108039.
[53] F. Abe, et al., CDF Collaboration, Phys. Rev. D 56 (1997) 3811.
[54] A.M. Poskanzer, S.A. Voloshin, Phys. Rev. C 58 (1998) 1671, arXiv:nucl-ex/9805001.
[55] A. El, I. Bouras, F. Lauciello, Z. Xu, C. Greiner, arXiv:1103.4038 [hep-ph].
[56] I. Bouras, E. Molnar, H. Niemi, Z. Xu, A. El, O. Fochler, C. Greiner, D.H. Rischke, Phys. Rev. Lett. 103 (2009) 032301, arXiv:0902.1927 [hep-ph].